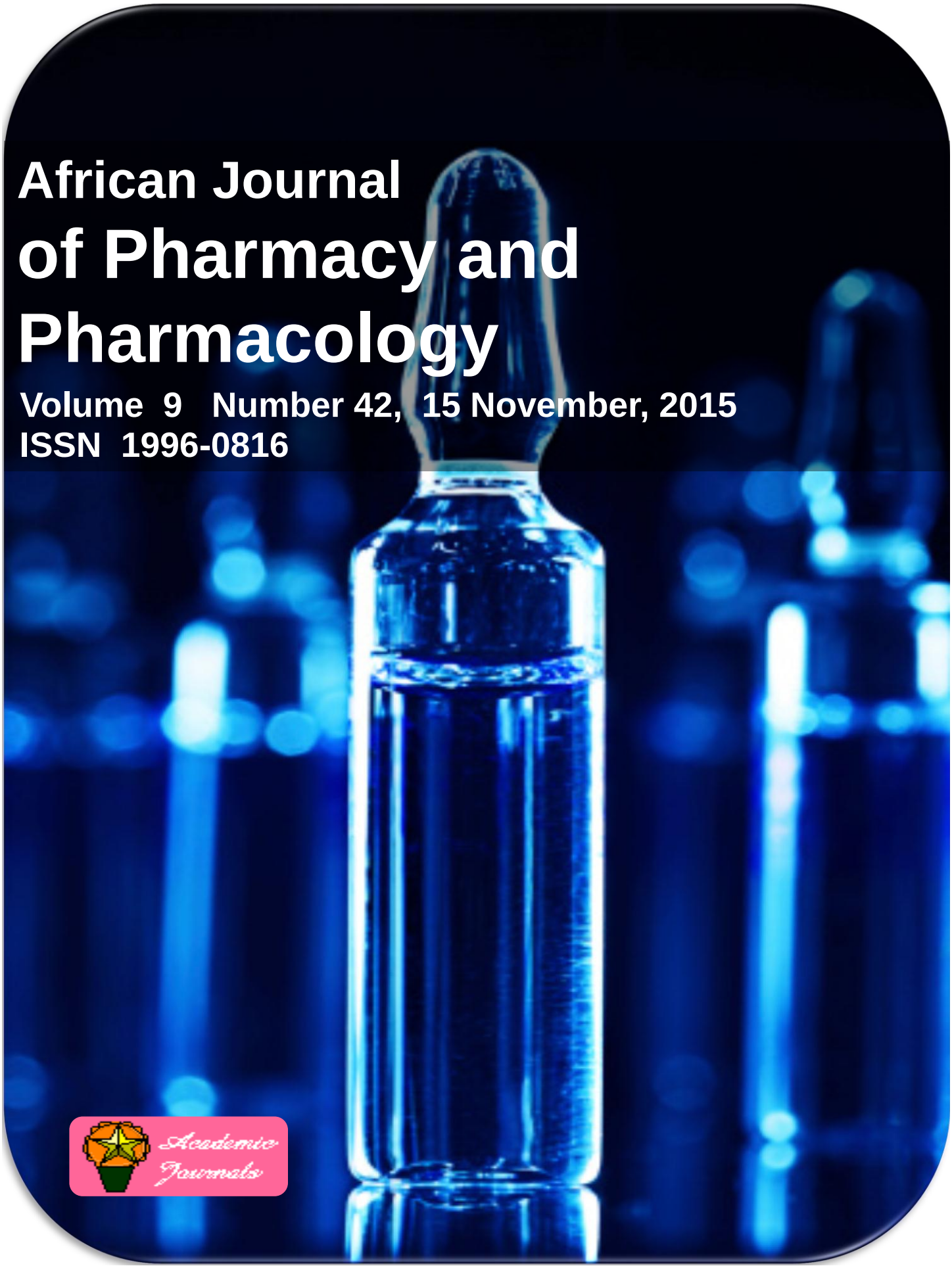

African Journal of Pharmacy and Pharmacology

Volume 9 Number 42, 15 November, 2015
ISSN 1996-0816

Academic Journals

ABOUT AJPP

The **African Journal of Pharmacy and Pharmacology (AJPP)** is published weekly (one volume per year) by Academic Journals.

African Journal of Pharmacy and Pharmacology (AJPP) is an open access journal that provides rapid publication (weekly) of articles in all areas of Pharmaceutical Science such as Pharmaceutical Microbiology, Pharmaceutical Raw Material Science, Formulations, Molecular modeling, Health sector Reforms, Drug Delivery, Pharmacokinetics and Pharmacodynamics, Pharmacognosy, Social and Administrative Pharmacy, Pharmaceutics and Pharmaceutical Microbiology, Herbal Medicines research, Pharmaceutical Raw Materials development/utilization, Novel drug delivery systems, Polymer/Cosmetic Science, Food/Drug Interaction, Herbal drugs evaluation, Physical Pharmaceutics, Medication management, Cosmetic Science, pharmaceuticals, pharmacology, pharmaceutical research etc. The Journal welcomes the submission of manuscripts that meet the general criteria of significance and scientific excellence. Papers will be published shortly after acceptance. All articles published in AJPP are peer-reviewed.

Submission of Manuscript

Submit manuscripts as e-mail attachment to the Editorial Office at: ajpp@academicjournals.org. A manuscript number will be mailed to the corresponding author shortly after submission.

The African Journal of Pharmacy and Pharmacology will only accept manuscripts submitted as e-mail attachments.

Please read the **Instructions for Authors** before submitting your manuscript. The manuscript files should be given the last name of the first author.

Editors

Editorial Board

African Journal of Pharmacy and Pharmacology

Table of Contents: Volume 9 Number 42 15 October, 2015

ARTICLES

Research Articles

academicJournals

Vol. 9(42), pp. 1002-1008, 15 November, 2015
DOI: 10.5897/AJPP2015.4408
Article Number: B4DCA3256131
ISSN 1996-0816

http://www.academicjournals.org/AJPP

African Journal of Pharmacy and Pharmacology

Full Length Research Paper

Gender-related differences in pharmacokinetic parameters of tramadol following intravenous and subcutaneous administration in dogs

Buhari Salisu[1]*, Kalthum Hashim[2], Goh Yong Meng[3] and Gan Siew Hua[4]

[1]Department of Veterinary Surgery and Radiology, Faculty of Veterinary Medicine, Usmanu Danfodiyo University Sokoto, Nigeria.
[2]Faculty of Veterinary Medicine, Universiti Malaysia Kelantan, 16100 Kota Bharu Kelantan, Malaysia.
[3]Department of Veterinary Preclinical Studies, Faculty of Veterinary Medicine, Universiti Putra Malaysia, 43400 UPM Serdang, Selangor, Malaysia.
[4]Human Genome Centre, School of Medical Sciences, Universiti Sains Malaysia, 16150 Kubang Kerian Kelantan, Malaysia.

Received 12 July, 2015; Accepted 21 October, 2015

The kinetics of tramadol at 3 mg/kg was studied in twenty four local dogs (twelve males and twelve females), after a single intravenous and subcutaneous dose administration. Three milliliters of blood from the jugular vein were collected before and at 2, 5, 10, 15, 30 and 45 min, 1, 1.5, 2, 2.5, 3, 4, 6, 8 and 9 h post administration of tramadol from both groups with the exception of 2 min for subcutaneous group. The collected blood samples were analyzed using a high performance liquid chromatography. In male dogs, the maximum plasma concentration (Cmax) was attained (Tmax) much faster (0.17 h) and systemic bioavailability was higher (29.65±11.7%) than in female dogs with 15.68±4.19%. On the other hand, AUC, $t_{1/2\alpha}$, $t_{1/2\beta}$ $Vd_{(ss)}$ were not significantly different between male and female dogs. These findings suggest the presence of some differences in the kinetics of tramadol between the male and female dogs.

Key words: Tramadol, pharmacokinetics, gender-difference, dogs.

INTRODUCTION

Gender is the most important factor in mammalian development and response to exogenous agents (Maris et al., 2010). The common surgical procedure is ovariohysterectomy and involves female dogs (Kongara et al., 2010) hence male dogs are underrepresented. Unequal representation of male dogs in frequent surgical and clinical trials has caused a relative paucity of data toevaluate possible gender differences in tramadol pharmacokinetics. Gender differences in the pharmacokinetics of some drugs are known to exist

*Corresponding author. E-mail: msbuhari7@gmail.com.

(Franconi et al., 2007; Soldin and Mattison, 2009). Evaluation of these gender differences is of clinical importance in designing effective post-surgical p pain management protocols. In dogs, unlike in rats (Liu et al., 2003) and humans (Ardakani and Rouini, 2007), gender dependency of pharmacokinetics of tramadol has not been investigated in detail. Recent clinical and *in vitro* evidence related the higher expression of cytochrome P450 (CYP) 3A4 in females (Lamba et al., 2010; Yang et al., 2010) to gender related differences. Furthermore, gender related difference in systemic exposure and related pharmacokinetic parameters of tramadol enantiomers were reported among Chinese volunteers (Hui-chen et al., 2004). The high variability in the tramadol pharmacokinetic properties was partly related to CYP2D6 and MDR1 polymorphism. Variation within the extensive metabolizer phenotype based on the number of functional alleles was observed. CYP2D6 activities were reported to be higher in males than in females, leading to higher Cmax and AUC of the metabolites (M1) (Ardakani and Rouini, 2007). Contrary to that, Hui-chen et al. (2004) found higher values in females than in male volunteers. The main objective of this study was to determine whether pharmacokinetic parameters of tramadol differed in male and female dogs.

MATERIALS AND METHODS

Twenty four local dogs of both sexes; twelve males weighing between 15 and 22 kg (average 18.5±2.2 kg), and twelve females of between 12.5 and 18 kg (average 15.75±1.9 kg), aged between 1.5 and 4 years (mean 2.92±0.82 years), and aged between 1.5 and 3 years (mean 2.33±0.6) years were used for the study. They were obtained and kept separately, and were certified healthy based on physical and clinical examination prior to the study. On the morning of study, a 20 gauge $1_{1/4}$ inch sterile catheter (Terumo, Somerset NJ, USA) was placed and secured in the cephalic vein. A baseline 2 ml venous blood sample was collected from each dog before tramadol administration. The dogs were randomly divided into four groups of equal number and were fasted for 12 h prior to beginning of the study but had access to water until two hours to tramadol administration. Group I and II are male dogs and received 3 mg/kg tramadol intravenously and subcutaneously respectively while III and IV are female dogs also received 3 mg/kg tramadol intravenously and subcutaneously respectively. The experimental procedures were approved by the Universiti Putra Malaysia Animal Care and Utility Committee (UPM/FPV/PS/3.2.1.551/AUP-R86).

Sample collection for pharmacokinetic analysis

An 18 gauge jugular catheter was placed in each dog approximately 2 h prior to each study period. Three ml blood were taken before and at 2, 5, 10, 15, 30 and 45 min, 1, 1.5, 2, 2.5, 3, 4, 6, 8 and 9 h post administration of tramadol from groups with exception 2 min among the subcutaneous groups. Prior to removing blood samples for pharmacokinetic analysis, 1 ml sample of blood was removed from the jugular catheter and discarded. Catheters were flushed with 1 ml of sterile saline following each sample collection. Samples were placed in a plane tube (Becton Dickinson, Franklin Lanes, New Jersey, USA) and allowed to stand at room temperature for 30 min to clot before immediately placed on ice. Samples were carefully and accurately labeled using a permanent marker. The blood samples were centrifuged at 1000 × g for 10 min, and the separated serum samples were kept frozen at -80°C until analysis within 6 months.

Serum tramadol extraction using solid phase extraction (SPE) method

Serum extraction was accomplished with disposable non-end-capped solid phase extraction cartridges. The columns were conditioned with 1 ml methanol, followed by 1 ml of diionised distilled water (DDH_2O). One milliliter of serum sample was loaded into each column. The columns were washed three times with 1 ml of DDH_2O, followed by washing with 250 µl of acetonitrile (ACN):ethylacetate (EtAc) (60:40) combination for three times. Columns were eluted four times with 250 µl of the mixture of ACN: EtAc (60:40) with added Triethylamine 1%. The eluent were collected into 10 ml falcon tubes and a volume of 50 µl of phenacetin was spiked from a 20 µg/ml working solution as an internal standard. The mixture was vortexed and dried under nitrogen stream heated to 40°C to facilitate evaporation. The sample was reconstituted in 70 µl of mobile phase and then filtered through a 4 mm nylon syringe filter, 0.4 µm before being injected into the high performance liquid chromatography (HPLC) system.

Serum tramadol assay using HPLC

Serum tramadol was analyzed by reverse phase HPLC with ultraviolet (UV) detection. High performance liquid chromatography is flexible and sensitive and can detect the tramadol at lower doses and from very small samples, which is really useful in clinical trials (Gan et al., 2002). Detection limit with HPLC was found to be as low as 20 ng/ml (Kukanich and Papich, 2004). The repeatability of the method for tramadol estimation reflects its precision in determining tramadol biotransformation (Gan et al., 2002). In a study on normal dogs Kongara et al. (2009) demonstrated the repeatability of HPLC for tramadol assay. Also, a large number of trials that used HPLC for quantitation of tramadol demonstrated the reliability of the method (Kukanich and Papich, 2004; Kubota et al., 2008). The HPLC system consisted of a quaternary pump, degasser, automated sampler, and UV detector which was set at 218 nm. The analytical column was Agilent Zorbax reverse phase, with a particle size of 5 µm and diameter and length of 4.6 x 250 mm. The control of the HPLC system and data collection was achieved by use of an IBM-compatible computer equipped with Agilent LC ChemStation software. The HPLC method was based on previously published study (Gan and Ismail, 2001). To achieve separation, the Agilent Zorbax RP-C18 column was heated to 40°C. The mobile phase was a mixture of 70% phosphate buffer (0.01 M), 30% acetonitrile with addition of 0.1% triethylamine (v/v), and adjusted to a pH of 5.9. The phosphate buffer was prepared fresh daily by dissolving 1.36 g of KH_2PO_4 (HPLC grade, Fisher Scientific Loughborough, Leicestershire LE11 5RG UK) into 1000 ml DD H_2O. The final mixture was filtered under vacuum through a 0.45 µm cellulose filter (Sartorius, Germany) and sonicated for 20 min. A flow-rate of 0.75 ml/min was chosen and an injection volume of 25 µl for each reconstituted sample throughout.

Standard curve for tramadol

Standard curves for tramadol were prepared daily. The pure

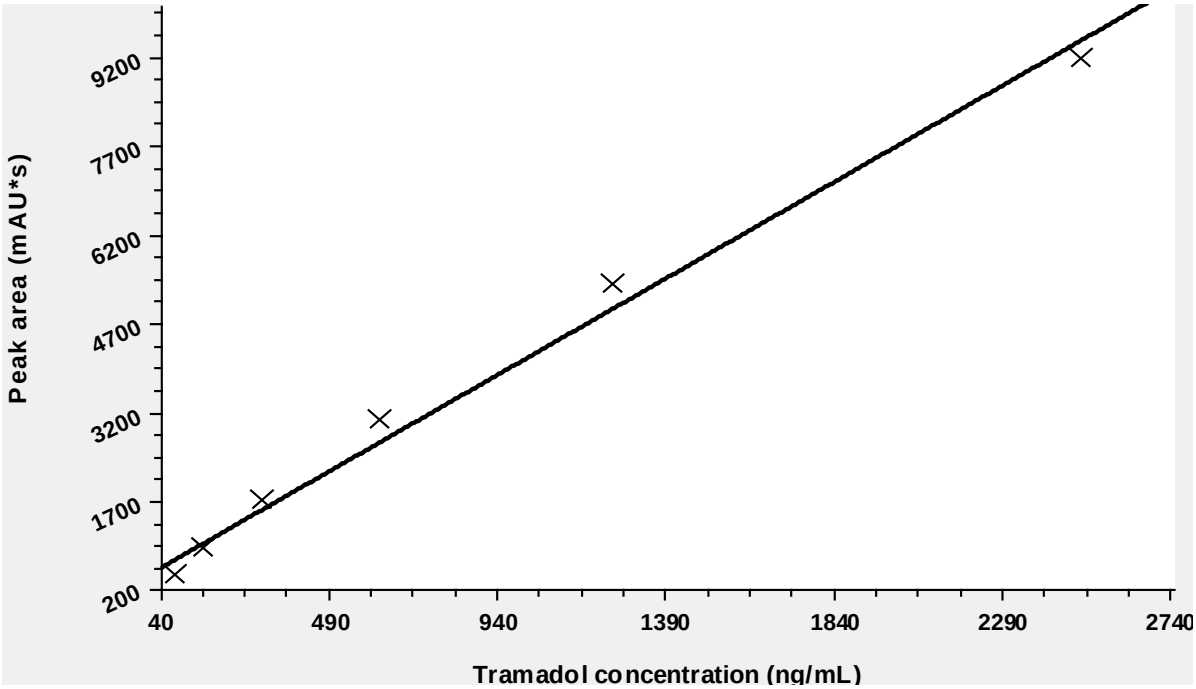

Figure 1. Graph of known concentrations of tramadol range from 40 to 2500 ng/ml (X-axis) plotted against peak area (Y-axis) determined (r = 0.99).

dry tramadol (Sigma-Adrich Co., 3050 Spruce Street, St. Louis, M063103 USA) was diluted in mobile phase to produce a concentration range from 40 to 2500 ng/ml and directly injected into the HPLC system for analysis. Daily calibration with a coefficient of determination (r^2) value greater than 0.99 was accepted.

Preparation of daily quality control samples

Quality control samples were prepared and run daily before injecting experimental sample. Canine frozen serum samples were left on the bench to thaw naturally and were vortexed prior to use. The curves were prepared by fortifying pooled canine serum with pure dry tramadol to produce a concentration range from 40 to 2500 ng/ml, while phenacetin was added at 20 µg/ml throughout. Preparation and processing of the fortified calibration samples were exactly as described for the incurred serum samples.

Pharmacokinetic analysis

Pharmacokinetic variables of tramadol following administration were calculated using a pharmacokinetic computer software program (WinNonlin 6.2.1. Pharsight Corp., Mointain View CA, USA). A weight factor of ($1/y^2$) was applied to the pharmacokinetic calculations. The best fit model for compartmental analysis was determined by residual plots and Aikake's information criterion. An open two-compartment model with central compartment best described the decline in tramadol plasma concentration following intravenous administration, and a standard non-compartmented model following subcutaneous administration. Values for total body clearance (Cl), volume of distribution (Vd), area under the plasma concentration curve (AUC), plasma distribution half-life a ($aT_{1/2}$), plasma clearance half-life b($b\ T_{1/2}$), intercept of the distribution phase (A), intercept of the elimination phase (B), rate constant associated with distribution (alpha), and rate constant associated with elimination (beta) were derived.

Statistical analysis

Statistical analysis was performed using the SPSS program (IBM® SPSS software Inc. version 16, New York, USA). The results are expressed as the means ± SD. The pharmacokinetic parameters were compared using an independent *t*-test between the groups. A *p*-value of less than 0.05 was considered to be statistically significant.

RESULTS

The linear concentration range for tramadol analysis was 40 to > 2500 ng/ml (39.625, 78.125, 156.25, 312.5, 625, 1250, 2500) ng/ml, (n = 5) (r^2 > 0.99). The limit of detection and quantitation were found to be 10 and 50 ng/ml respectively (Figure 1). Mean retention time for phenacetin (internal standard) was 6.98 min (Figure 2) and tramadol was 5.09 min (Figure 3). Dog experimental tramadol plasma chromatogram 5 min and 6 h after administration are presented in Figures 4 and 5 respectively.

No adverse effects were observed after administration of tramadol HCl at 3 mg/kg. All dogs appeared mildly sedated after administration and a dog showed sign of nausea (salivating) but stopped after about 5 min. A female dog became very aggressive and was replaced with another female dog.

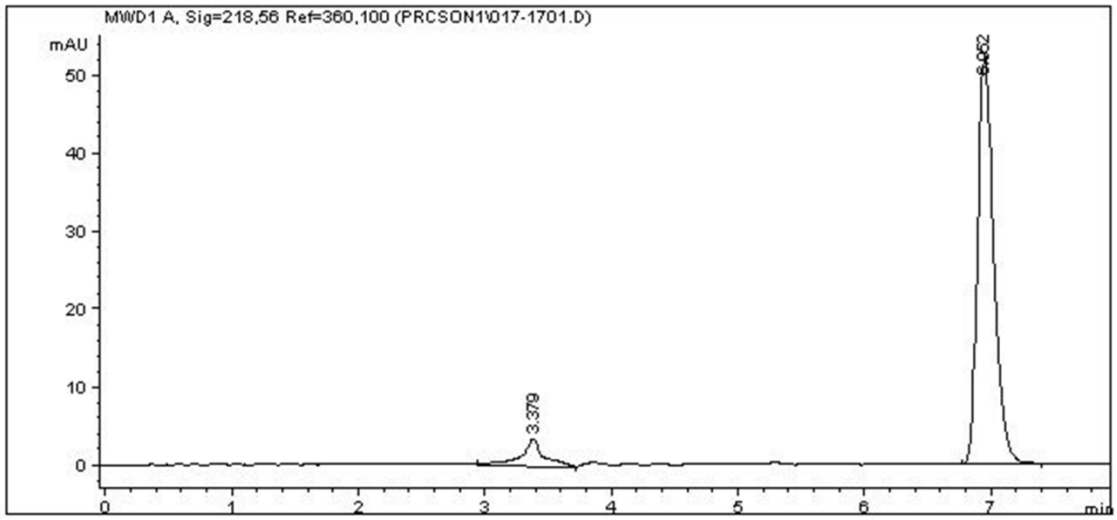

Figure 2. Representative chromatogram obtained from phenacetin injected into HPLC at 20 µg/mL as an internal standard.

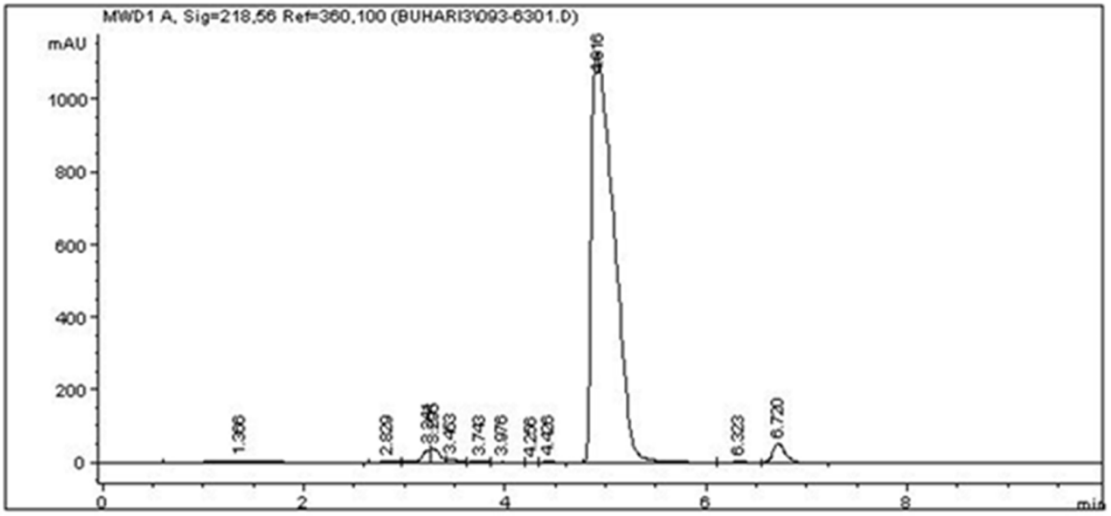

Figure 3. Representative chromatogram obtained from tramadol and phenacetin injected into HPLC at 5000 and 20 µg/ml, respectively.

Influence of gender on pharmacokinetic of tramadol in dogs

Similar results were obtained after tramadol pharmacokinetic analysis for gender difference subgroups. However, it is interesting to note that systemic bioavailability was higher among the male dogs (29.65±11.7%) than female dogs with 15.68±4.19%. This resulted to a significantly higher rate of movement from compartment 1 to compartment 2 among the female dogs (13.34±12.58 l/h) than the male dogs (5.99±4.1 l/h). Maximum plasma concentration (Cmax) was attained (Tmax) much faster (0.17 h) among the male dogs compare to the female dogs (0.75 h). On the other hand, AUC, $t_{1/2\alpha}$, $t_{1/2\beta}$ $Vd_{(ss)}$ were not significantly different between male and female dogs. These findings suggest that the tramadol is influenced to a lesser extent by gender differences. The pharmacokinetic parameters are summarized in Table 1.

DISCUSSION

The gender related pharmacokinetic parameters derived

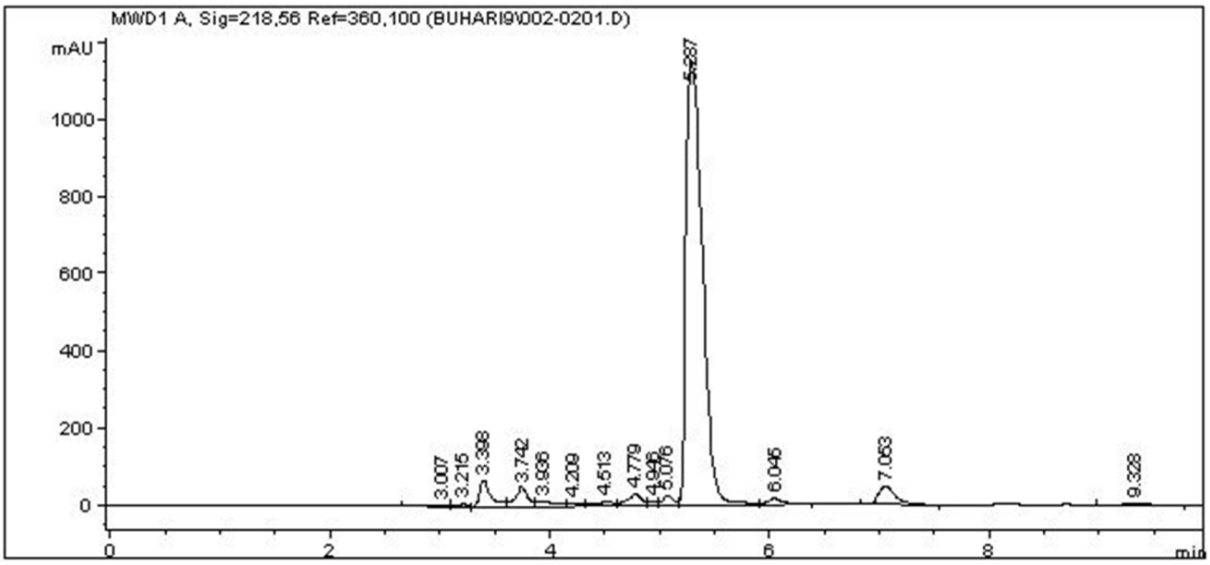

Figure 4. Tramadol plasma representative chromatogram obtained from dog 5 min following administration.

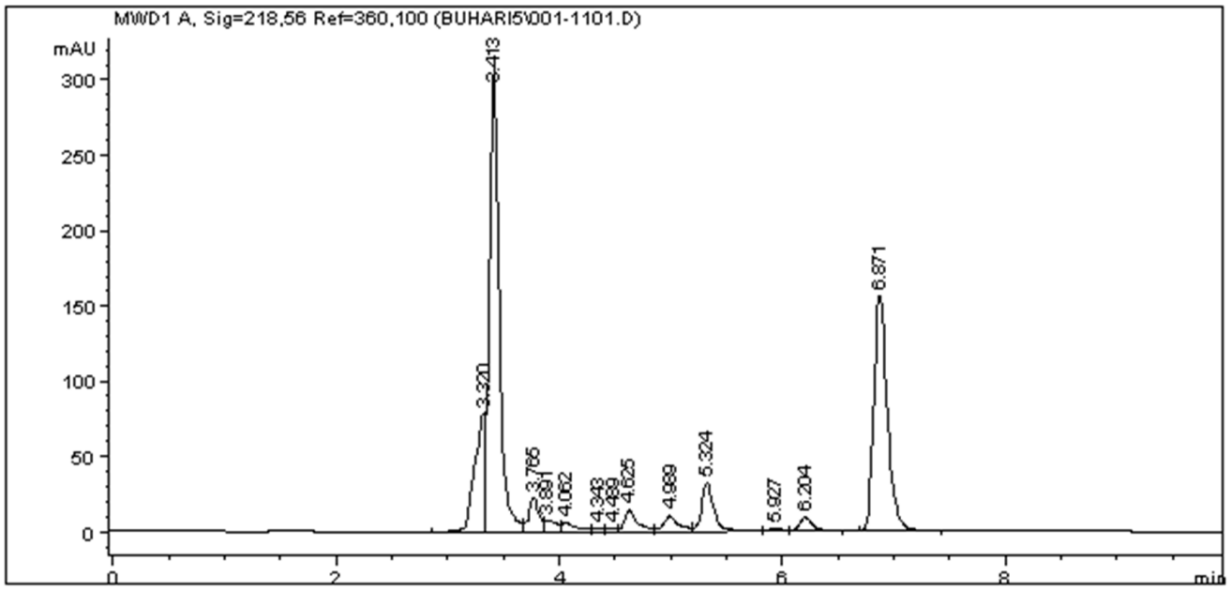

Figure 5. Tramadol plasma representative chromatogram obtained from dog 6 h following administration.

for tramadol in our study differ somewhat to those recently published by Cagnardi et al. (2011) in cats. Our results showed a significantly faster time to reach high plasma tramadol concentration (0.17 ± 0.01 h) in male dogs compare with relatively slower (0.75±0.01 h) among the female dogs. Rate of movement of tramadol from first compartment to the second compartment was significantly lower (5.99±4.1) in the male dogs compare with 13.34±12.58 found among the female dogs, and subsequently higher systemic bioavailability (29.65±11.7%) among the male dogs versus lower values (15.68±4.14%) observed in the female dogs. However, a wide inter-individual variation was observed among the female dogs (range from 11.3 to 24.4%). Unlike Cagnardi et al. (2011) who reported no sex-related differences in tramadol pharmacokinetics in cats and Ardakani and Rouini (2007) among human volunteers. Hui-chen et al. (2003) observed a significant gender variation in pharmacokinetics of trans-tramadol in rats. However, they observed systemic exposure among the female rats compared with the male rats. In another study by Djurendic-Brenesel et al. (2010), significantly higher

Table 1. Pharmacokinetic parameters of tramadol (Mean ± SD) following intravenous (3 mg/kg) and subcutaneous (3 mg/kg) administration in both male and female dogs.

Parameter	Group I (n = 6)	Group II (n = 6)	Group III (n = 6)	Group IV (n = 6)
A (ng/ml)	195.07±40.82[a]	NA	657.3±462.5[b]	NA
B (ng/ml)	173.13±23.93	NA	148.68±47.28	NA
α (l/h)	11.42±3.8[a]	NA	45.61±39.19[b]	NA
β (l/h)	1.13±0.29	NA	1.12±0.2	NA
λz (l/h)	1.23±0.44	0.65±0.16[a]	1.43±0.21	1.09±0.37[b]
$t_{1/2}$λz (h)	0.58±0.16	1.13±0.34[a]	0.49±0.07	0.69±0.21[b]
$t_{1/2\alpha}$ (h)	0.07±0.03	NA	0.04±0.04	NA
$t_{1/2\beta}$ (h)	0.65±0.16	NA	0.64±0.11	NA
C_0 (ng/ml)	294.17±22.68[a]	NA	333±120.48[b]	NA
Cmax (ng/ml)	245.57±26.02[a]	NA	127.16±18.69[b]	NA
Tmax (h)	0.17±0.01[a]	NA	0.75±0.01[b]	NA
MRT (h)	0.85±0.22[a]	1.52±0.37[b]	0.76±0.18[a]	1.39±0.19[b]
Cl_T (mL/min/kg)	17.71±5.02	17.17±4.32	21.06±9.34	16.53±5.29
$Vd_{(ss)}$(L/kg)	14.18±1.56	NA	14.37±4.96	NA
$AUC_{0-\infty}$ (h*ng)/ml	179.52±44.47	177.19±63.28	177.61±85.16	196.01±57.66
$AUMC_{0-\infty}$ (h*h*ng)/ml	159.34±75.85[a]	276.21±81.44[b]	140.01±75.25[a]	281.05±11.75[b]
K10 (l/h)	2.54±1.07	NA	4.33±2.1	NA
K12 (l/h)	5.99±4.1[a]	NA	13.34±12.5[b]	NA
K21 (l/h)	7.61±2.97	NA	6.12±1.46	NA
K10 $t_{1/2}$ (h)	0.34±0.12	NA	0.17±0.1	NA
V1 (L/kg)	7.7±1.62	NA	3.3±2.93	NA
V2 (L/kg)	5.91±1.74	NA	8.92±2.81	NA
F (L/kg)	NA	29.65±11.7[a]	NA	15.68±4.19[b]

[a,b]means with different superscripts within rows different significantly at p=0.05.

Abbreviations: Group I = male dogs treated with a single dose of 3 mg/kg tramadol intravenously; Group II = male dogs treated with a single dose of 3 mg/kg tramadol subcutaneously; Group III = female dogs treated with a single dose of 3 mg/kg tramadol intravenously; Group IV = female dogs treated with a single dose of 3 mg/kg tramadol subcutaneously; NA not applicable; λz = first-order rate constant; t½ λz = half-life of the terminal portion of the curve; MRT = mean residence time; Cl_T = total body clearance; Vdss = volume of distribution at steady state; AUC0-∞ = area under the curve from 0 to infinity; AUMC0-∞ = area under the first moment curve from 0 to infinity; CO = concentration at time 0; Cmax = maximum concentration; tmax = time to maximum concentration; t½α = distribution half-life; t½β = elimination half-life; α = rate constant associated with distribution; β = rate constant associated with elimination; A = intercept for the distribution phase; B = intercept for the elimination phase; K10 = elimination rate from compartment 1; K12 = rate of movement from compartment 1 to compartment 2; K21= rate of movement from compartment 2 to compartment 1; K10 $t_{1/2}$ = half-life of the elimination phase; V1= volume of compartment 1; V2 = volume of compartment 2; F = bioavailability.

plasma opiates were measured among male rats over the female rats. This finding is in concordance with our observation, suggesting a faster passage of the drug from blood to the organs in female dogs. Gender relatedvariability in the pharmacokinetic properties of tramadol has been partly related to CYP2D6 and MDR1 polymorphism in humans. In addition, variation within population of extensive metabolizers (EM) phenotype was observed based on number of functional CYP2D6 alleles (Ardakani and Rouini, 2007). The activity of CYP2D6 has been reported to be higher in males than in females (Tanaka, 1999). Contrary to this, Hui-chen et al. (2004) reported a higher rate of O-demethylation of tramadol mediated by CYP2D6 resulting in higher Cmax and AUC in females over the males volunteers.

Both distribution and elimination half-lives remain unaffected, and volumes of distribution and elimination rates were not significantly different between the gender groups. This is similar to the observation made by Cagnardi et al. (2010) in cats, and in accordance with Ardakani and Rouini (2007) among human volunteers.

Conclusion

In conclusion, the clinical implications of these findings seem clear. If the aim is to achieve similar analgesic plasma levels of tramadol among male and female dogs it is unwise to give equal dose; not only that it takes faster time to reach high plasma tramadol concentration in male dogs but higher systemic bioavailability among the male dogs is achieved. If analgesia is to be achieved with tramadol administration, adjustment in the dose rate would have to be made to compensate for the poor bioavailability of the drug in female dogs. Overall, we conclude that there were some differences in the kinetics

between the male and female dogs.

Conflict of Interests

The authors have not declared any conflict of interests.

REFERENCES

Ardakani YH, Rouini MR (2007). Pharmacokinetics of tramadol and its three main metabolites in healthy male and female volunteers. Biopharma Drug Disp. 28(9):527-534.

Cagnardi P, Villa R, Zonca A, Gallo M, Beccaglia M, Luvoni GC, Vettorato E, Carlis S, Fonda D, Ravasio G (2011). Pharmacokinetics, intraoperative effect and postoperative analgesia of tramadol in cats. Res. Vet. Sci. 90(3):503-509.

Djurendic-Brenesel M, Mimica-Dukic N, Pilija V, Tasic M (2010). Gender- related differences in the pharmacokinetics of opiates. Forensic Sci. Int. 794(1-3):28-33.

Franconi F, Brunelleschi S, Steardo L, Cuomo V (2007). Gender differences in drug responses. Pharmacol. Res. 55(2):81-95.

Gan SH, Ismail R (2001). Validation of a high-performance liquid chromatography method for tramadol and o-desmethyltramadol in human plasma using solid-phase extraction. J. Chromatogr. B Biomed. Sci. Appl. 759(2):325-335.

Gan SH, Ismail R, Wan Adnan WA, Wan Z (2002). Method development and validation of a high-performance liquid chromatographic method for tramadol in human plasma using liquid- liquid extraction. J. Chromatogr. B Analyt. Technol. Biomed. Life Sci. 772(1):123-129.

Hui-Chen L, Shu-Min J, Yong-Li W (2003). Gender-related differences in pharmacokinetics of enantiomers of trans-tramadol and its active metabolite, trans-O-demethyltramadol, in rats. Acta Pharmacol. Sin. 24(12):1265-1269.

Hui-chen L, Yang Y, Na W, Ming D, Jian-fang L, Hong-yuan X (2004). Pharmacokinetics of the enantiomers of trans-tramadol and its active metabolite, trans-O-demethyltramadol, in healthy male and female Chinese volunteers. Chirality 16(2):112-118.

Kongara K, Chambers JP, Johnson CB (2010). Electroencephalographic responses of tramadol, parecoxib and morphine to acute noxious electrical stimulation in anaesthetised dogs. Res. Vet. Sci. 88(1):127-133.

Kongara K, Chambers P, Johnson CB (2009). Glomerular filtration rate after tramadol, parecoxib and pindolol following anaesthesia and analgesia in comparison with morphine in dogs. Vet. Anaesth. Analg. 36(1):86-94.

Kubota R, Komiyama T, Miwa Y, Ide T, Toyoda H, Asanuma F, Yamada Y (2008). Pharmacokinetics and postoperative analgesia of epidural tramadol: A prospective, pilot study. Cur. Ther. Res. Clin. Exp. 69(1):49-55.

KuKanich B, Papich MG (2004). Pharmacokinetics of tramadol and the metabolite O-desmethyltramadol in dogs. J. Vet. Pharmacol. Ther. 27(4):239-246.

Lamba V, Panetta JC, Strom S, Schuetz EG (2010). Genetic Predictors of Interindividual Variability in Hepatic CYP3A4 Expression. J. Pharmacol. Exp. Ther. 332(3):1088-1099.

Maris AF, Franco JL, Mitozo PA, Paviani G, Borowski C, Trevisan R, Uliano-Silva M, Farina M, Dafre AL (2010). Gender effects of acute malathion or zinc exposure on the antioxidant response of rat hippocampus and cerebral cortex. Basic Clin. Pharmacol. Toxicol. 707(6):965-970.

Soldin OP, Mattison DR (2009). Sex Differences in Pharmacokinetics and Pharmacodynamics. Clin .Pharmacokinet 48(3):143-157.

Tanaka E (1999). Gender-related differences in pharmacokinetics and their clinical significance. J. Clin. Pharm. Ther. 24(5):339- 346.

Yang X, Zhang B, Molony C, Chudin E, Hao K, Zhu J, Gaedigk A, Suver C, Zhong H, Leeder JS, Guengerich FP, Strom SC, Schuetz E, Rushmore TH, Ulrich RG, Slatter JG, Schadt EE, Kasarskis A, Lum PY (2010). Systematic genetic and genomic analysis of cytochrome P450 enzyme activities in human liver. Genome Res. 20(8):1020-1036.

academicJournals

Vol. 9(42), pp. 1009-1019, 15 November, 2015
DOI: 10.5897/AJPP2015.4383
Article Number: 177D09B56137
ISSN 1996-0816

http://www.academicjournals.org/AJPP

African Journal of Pharmacy and Pharmacology

Full Length Research Paper

Synthesis of Cu(II) complex with schiff bases derived from aryl-*S*-benzyldithiocarbazate: Antimicrobial activity and *in silico* biological properties evaluations

K. G. O. Casas[1], M. L. G. Oliveira[2], G. D. de Fátima Silva[2], C. J. Viasus[3] and A. E. Burgos[1]*

[1]Grupo de Investigación en Química de Coordinación y Bioinorgánica, Departamento de Química, Facultad de Ciencias, Av. Carrera 30 # 45-03, Universidad Nacional de Colombia – Sede Bogotá, Colombia.
[2]Departamento de Química, Instituto de Ciências Exatas, Universidade Federal de Minas Gerais, Av. Antônio Carlos, 6627, CEP 31270-901, Belo Horizonte, Minas Gerais, Brazil.
[3]Grupo de Investigación en Compuestos de Coordinación y Catálisis, Facultad de Ciencia y Tecnología, Universidad de Ciencias Aplicadas y Ambientales, U. D. C. A., Sede Norte, Calle 72 # 14-20, Bogotá, Colombia.

Received 16 June 2015; Accepted 29 September, 2015

This study reported the synthesis of the new ligands, 3,4-methylenedioxybenzyl-*S*-benzyldithiocarbazate (L1), *p*-chloro-benzyl-*S*-benzyldithiocarbazate (L2) and 2,6-dichlorobenzyl-*S*-benzyldithiocarbazate (L3). These three schiff base type ligands were respectively obtained by means of the reaction of 3,4-methylenedioxybenzaldehyde, *p*-chlorobenzaldehyde and 2,6-dichlorobenzaldehyde with S-benzyldithiocarbazate, at molar ratio 1:1. The respective Cu(II) complex C1, C2 and C3 were synthesized by the reaction of L1, L2 or L3, with $CuCl_2.{}_2H_2O$, at molar ratio 1:1. The chemical identification of ligands and respective complexes was established through spectroscopic data (FT-IR, UV-Vis and ^{1}H NMR). The ligand and complexes were subjected to *in vitro* radial diffusion assays against the gram-negative bacteria *Escherichia coli* and gram-positive *Staphylococcus aureus* and the fungus *Candida albicans* and *Saccharomyces cerevisiae*, with good results for some of these compounds. Due to its promising antimicrobial property, complex C1 was subjected to EPR analyses aiming to establish its conformational structure. The prediction of biological activities of ligands and complexes were evaluated through the simulation carried out *in silico* using the web tools PASSonline and ChemMapper.

Key words: Aryl-*S*-benzyldithiocarbazate, Cu(II) complexes, antimicrobial activity, PASSonline, ChemMapper.

INTRODUCTION

In the last decades the coordination complex derived from *S*-benzyldithiocarbazate has been widely studied, mainly due to its activity against viruses, bacteria and fungus and as antitumor, pesticide and others (Tarafder et al., 2002a,b; Zangrando et al., 2015; Islam et al., 2014; Nanjundan et al., 2014). The presence in their structure

*Corresponding author. E-mail: aeburgosc@unal.edu.co.

of two electron-donors facilitates the coordination processes with metal ions involving nitrogen and sulfur atoms. This property makes these compounds even more interesting for the development of further studies involving biological and pharmacological activities (Garoufis et al., 2009).

Schiff bases are molecules used in the generation of supra molecular structures (Ziessel, 2001). This type of compounds are broad chemical and biological interest, mainly because of the possible ways of coordinating to the metal ion, the stability of the complexes which, in general present an increased activity compared to their respective free ligands (Ravoof et al., 2004; Ravoof et al., 2007; Monika et al., 2014). The shiff bases derived from alkyl-S-benzyldithiocarbazates obtained by the condensation of the an aldehyde or a ketone with dithiocarbazate, present different biological properties increasing the interest of researchers for this kind of ligands (How et al., 2008; Tarafder et al., 2001; Islam et al., 2011; Ali et al., 2012). To metallic complexes obtained reacting these ligands with Cd(II), Zn(II), Ni(II), Co(II), Sn(IV) or Cu(II) were attributed *in vitro* pharmacological activities such as antibacterial, antifungal, and inhibitory effect of the leukemia and ovarian cancer cell growth (Ali, 1997; Tarafder et al., 2002a,b; Islam et al., 2014; Nanjundan et al., 2014; Monika et al., 2014; Esmaielzadeh et al., 2014; Zangrando et al., 2015). And, studies involving schiff bases such as thiosemicarbazones, showed that the complexes often present greater pharmacological activity than the original free ligands. Thus, the study of these compounds becomes more important (Beraldo, 2004; Rigol et al., 2005).

In recent years, gold complexes have been used for the treatment of arthritis, silver complexes for alleviate antibacterial infections and platinum complexes have been used against cancer (Kelland, 2007; Ott, 2009; Chen et al., 2009; Alanne et al., 2013). In these and other cases, the complex has been more active than the original free ligand or may induce a lower cell drug resistance (Alanne et al., 2013). In addition, some side effects produced by ligands may also be reduced due to complexation with metals. However, to acquire greater knowledge about the biological effect of these compounds, it is necessary a long period of researches and the involvement of high financial resources. This fact makes it difficult or unfeasible to conduct more comprehensive studies to prove the true pharmacological potential of these compounds. A good alternative to selecting the first biological targets to be evaluated is the use of tools in which the chemical structure of the synthesized compounds is compared with the active compounds already known. In some situations, the use of these tools allows establishing structural similarities with known active compounds, and provides good starting point to investigate the potential pharmacological activity associated to specific compound.

The pharmacological effect or potential biological target, established by means of computer (*in silico*) tools can be further proven through experiments performed *in vitro* and/or *in vivo*. PASSonline (Prediction Activity Spectra of Substances) and ChemMapper represent a good examples of web tools that contain large amount of information available in open access databases.

The strategy of PASSonline web tool involves decomposition of chemical structure on topological structure superposition fragmental notation (SSFN) descriptors type. Then, this tool develops a comparison of these descriptors with about 250,000 data of drugs, drug candidates, compounds under registration processes, toxic substances, chemical oncogenes and other biologically active compounds (Lagunin et al., 2000; Filimonov et al., 2014). And, by means of Bayesian statistical methods, the potential pharmacologic and/or toxicological activities are established based on its relationships with similar compounds available on the base data. The final results are established in accordance with quantitative structure–activity relationship (QSAR) models (Lagunin et al., 2000; Lagunin et al., 2010).

The SHApe-FeaTureSimilarity (SHAFTS) is used in ChemMapper tool (Gong et al., 2013a) in which it was validated in relation to base data Directory of Useful Decoys (DUD-E) (Wang et al., 2014; Mysinger et al., 2012). In the ChemMapper analysis, the superposition of the tridimensional chemical structures of compounds, together with identification of potential pharmacophores, is used to estimate the potential biological effects of target compound (Gong et al., 2013b; Lu et al., 2011; Liu et al., 2011).

This study described the synthesis and characterization of the ligands methylenedioxide-benzyl-*S*-benzyldithiocarbazate (L1), *p*-chloro-benzyl-*S*-benzyldithiocarbazate (L2) and 2,6-dichloro-benzyl-*S*-benzyldithiocarbazate (L3) (Figure 1). These schiff base type ligands were used to produce the complex 3,4-methylenedioxybenzaldehyde-Cu(II) (C1), *p*-chlorobenzaldehyde-Cu(II) (C2) and 2,6-dichlorobenzaldehyde-Cu(II) (C3) (Figure 1). The ligand L1, L2 and L3 and its correspondent complex C1, C2 and C3 were subjected to antimicrobial assays against the bacteria *Escherichia coli* (gram-negative) and *Staphylococcus aureus* (gram-positive), and the yeast *Candida albicans* and *Saccharomyces cerevisiae*. And, the results of antimicrobial assays of ligands and complexes were compared with the data prediction made by means simulation carried out using the web tools PASSonline and ChemMapper.

MATERIALS AND METHODS

Synthesis of ligands L1, L2 and L3

The alkyl-*S*-benzyldithiocarbazates L1, L2 and L3 (Figure 1) were

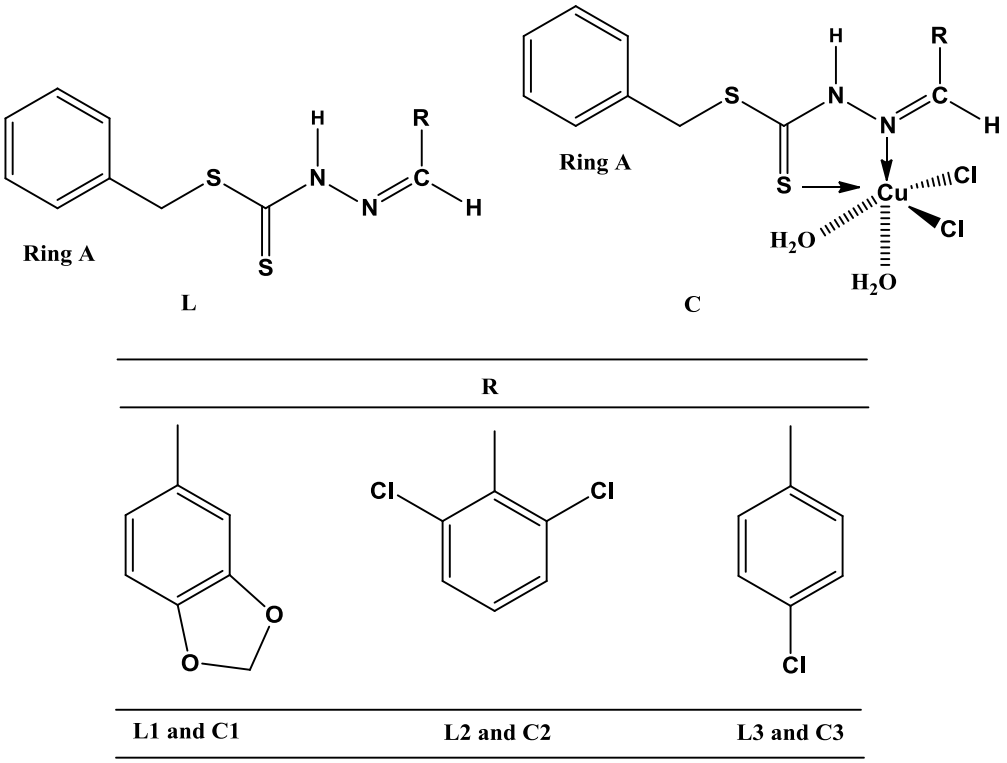

Figure 1. Chemical structures of 3,4-methylenedioxybenzyl-*S*-benzyldithiocarbazate (L1), *p*-chloro-benzyl-*S*-benzyldithiocarbazate (L2) and 2,6-dichlorobenzyl-*S*-benzyldithiocarbazate (L3), 3,4-methylenedioxybenzaldehyde-Cu(II) (C1), *p*-chlorobenzaldehyde-Cu(II) (C2) and 2,6-dichlorobenzaldehyde-Cu(II) (C3).

synthesized and purified in accordance with methodology suggested by Ali (1997) and Tarafdar (2001) together with its respective coworkers. Ethanol ≥ 99.8%, chloroform, 3,4-methylenedioxybenzaldehyde, *p*-chlorobenzaldehyde, 2,5-dichlorobenzaldehyde and $CuCl_2.2H_2O$ purchased were from Merck, Colombia. In the synthesis of ligands L1, L2 and L3 used aldehyde and *S*-benzyldithiocarbazate ratios as shown in Table 1.

The aldehyde used in each reaction was firstly dissolved in ethanol (5 ml) and mixed with *S*-benzyldithiocarbazate also dissolved in ethanol (5 ml). The mixture was kept under reflux at 78°C, with constant magnetic stirring for 2 h. Then, the solution was slowly cooled. The solvent was withdrawn in a Buchi rotavapor® under reduced pressure. After filtration this solid was washed with hot ethanol (3x 15 ml) and kept under vacuum in desiccators, protected against sun light. Each obtained solid L1 (yellow), L2 (yellow) and L3 (light yellow) was respectively cleaned with hexane (3x 15 ml), dried and kept under vacuum in desiccators over anhydrous calcium chloride, protected against sun light.

Synthesis of Cu(II)-complex C1, C2 and C3

The reactant $CuCl_2.2H_2O$ was dissolved in $CHCl_3$: MeOH (1:1) (10 ml) and then, it was added the ligand dissolved in a sufficient quantity of $CHCl_3$. The reaction mixture was kept under reflux at 68°C, with constant magnetic stirring for 2 h, carefully protected against sun light. The solvent was withdrawn in a Buchi rotavapor® under reduced pressure. Thus, the brown solid formed was washed with $CHCl_3$, dried and then kept under vacuum in desiccators, protected against sun light. The following conditions ratios were used in the synthesis of complex C1, C2 and C3 as shown in Table 2

Compound characterization

The chemical characterization of compounds was realized by means of physicochemical techniques. The fourier transform infrared (FTIR) spectra were obtained (1% KBr pellet) on SHIMADZU IR Prestige21 FTIR Spectrometer, with absorption band ranging from 4000 a 400 cm^{-1}. The ultraviolet spectra (UV) were performed at Thermo Scientific Evolution 300 UV-VIS spectrophotometer (280 to 900 nm), using quartz cuvette with 1 cm optical path. The sample was dissolved in Dimethyl Sulfoxide (DMSO), at concentration of $1x10^{-3}$ mol/L. The nuclear magnetic resonance of hydrogen (^1H NMR) spectra of ligand was recorded on Bruker AVANCE DRX-400 spectrometer (400 MHz). The ligand was dissolved in deuterated solvent DMSO-d_6 and $CDCl_3$ and TMS used as internal standard ($\delta_H = \delta_C = 0$). The molar conductance values of the 10^{-3}M DMSO solutions of the complexes were measured with a Hanna conductivity meter HI 5321. The electron paramagnetic resonance (EPR) was performed at room temperature on Bruker ESP300 Electron Spin Resonance ESP300-E X-band-Spectrometer, *g*-values were obtained from $g=h\nu/\beta H$, β is the Bohr magneton, *h* the Planck constant, ν is the frequency and *H* is the centers field at which the resonance occurs. The *g*-value is often a key parameter in identifying paramagnetic centers in a particular symmetry.

Antimicrobial activity

The bacteria *E. coli* (ATCC 25922) (gram-positive) and *S. aureus* (ATCC 292139) (gram-negative), and the yeasts *C. albicans* (ATCC 10231) and *S. cerevisiae* (ATCC AH22) were used to evaluate the

Table 1. Aldehyde and *S*-benzyldithiocarbazate ratios.

Reactants proportion				
Aldehyde	**mMol**	**mg**	***S*-benzyldithiocarbazate**	
			mMol	**mg**
3,4-Methylenedioxybenzaldehyde	0.36	54.0	0.36	67.0
p-Chlorobenzaldehyde	0.5	75.5	0.5	100.0
2,5-dichlorobenzaldehyde	0.5	87.5	0.5	101.0

antimicrobial activity of synthesized ligands and its respective Cu(II)-complex. The antimicrobial assays were performed using the disk diffusion method (Bauer and Kirby, 1966; Tamayo et al., 2014). The solution of microorganism (1.0 ml) with 600 nm optical density (OD_{600}) ranging from 0.1 to 0.2 was added to Petri plates. As culture medium, trypticase soja Agar (TSA) was added for bacteria and potato dextrose Agar (PDA) for the yeasts. Cefalothin (40.0 mg/ml) for bacteria and clotrimazole (1.0 %) for yeasts were used as positive control. Standard solutions (300.0 µg/ml) of ligands and complexes were prepared from stock solutions. Then, 20.0 µL of ligand L1, L2 or L3 and of the Cu(II) complex C1, C2 or C3 was added on culture medium. The microorganism susceptibility to each compound was determined by means of the growth inhibition halo (mm) and the minimum inhibitory concentration (MIC) was determined in µg/mL. The assays were performed in triplicate considering the median ± standard deviation of the mean (s.e.m.).

In silico tools used to evaluate biological activity

The chemical structures of ligand L1, L2 and L3, and the Cu(II)-complex C1, C2 and C3 (Figure 1) were built using the software ChemDraw® (version 12.0.2.1076, Cambridge Soft) and saved in MDL SDfile (*.SDF). The chemical structures were evaluated using the ChemMapper and PASSonline tools between days 5-15/September/2015.

PASSonline

To develop studies by means of PASSonline it is necessary to upload sdf file of the structure of compound. The PASSonline tool realizes the decomposition of structure in descriptors and a comparison with descriptors of biologically active substances available in its data base. The ligand L1, L2 and L3, and its (CuII)-complex C1, C2 and C3 were compared with more than 250,000 compounds, including drugs, potential drugs, compounds under register processes, toxic substances, oncogenes and other biologically active compounds ((Lagunin et al., 2000; Lagunin et al., 2010).

Simultaneously this tool develops predictions of different biological activities for the structure of organic compound, correlating the probability "to be active" (Pa) with probability "to be inactive" (Pi). Pa represent the probability that the studied compound is belonging to the sub-class of active compounds (resembles the structures of molecules, which are the most typical in a sub-set of "actives" in PASS training set). Pi represent the possibility that the studied compound is belonging to the sub-class of inactive compounds (resembles the structures of molecules, which are the most typical in a sub-set of "inactives" in PASS training set). At the end of analytical process, the results were established by difference (Pa–Pi), and the potential biological activities generated for ligands and complexes were organized in Table 6.

ChemMapper

The ligands L1, L2 and L3 and complexes C1, C2 and C3 also were analyzed using the ChemMapper tool. The predictions of biological activities for these compounds were established by means of the following base data (active compounds): PDB (7072), KEGG (5928), Drug Bank (4.645), ChEMBL (339.624) and BindingDB (364.221). The similarity score suggested by this tool were converted in percent of similarity with the compounds of the data base (1.2 similarity score = 0.6 % similarity). In the present study, the results of the similarity indices obtained through ChemMapper were converted in percent of similarity in the range of 0 to 1.0. The normalized values (score) presented by the tools were not used. The maximum values selected for the similarity score for the same target were considered only when it is > 60 % similarity. The profile of L1, L2 and L3 and C1, C2 and C3 was analyzed both in terms of chemical structure, such as in relation to the type of molecule superposition, correlating the average number of pharmacophores found in each one, as well as the same function in terms of similarity of the spatial conformation. At the end of analytical process applied to the compounds, the potential biological targets generated by this tool were organized in Table 7.

RESULTS AND DISCUSSION

The FTIR spectrum of the L1, L2 and L3 present characteristic absorption band of alkyl-S-benzyldithiocarbazate as reported by Ali and Tafafder (1997). In the spectrum, was observed strong absorption band at 3177 cm^{-1} that corresponds to the ν(N-H) of NH2 group present on the free ligand (Ali and Tafafder, 1997; Silverstein and Webster, 1997). In aqueous solutions, the ligand L1, L2 and L3 present a thione-thiol tautomerism which is brought due to the presence of thioamide NH–C=S functional group (Beckford et al., 2011). The absence in the IR spectra of absorption band at 2600 cm^{-1}, attributed to sulfhydryl group stretch (νS-H), and the presence of band at 940 to 970 cm^{-1} characteristic of C=S stretch, indicated that these ligands has in thione form, typical of similar compounds in solid state (Beckford et al., 2011; Tamayo et al., 2014). The schiff base derivatives also present strong absorption bands at 1597 cm^{-1} (L1 and L2) and 1577 cm^{-1} (L3) (Table 3). These are assigned to the ν(C-N) modes for the free ligand. In metal complexes, this band is shifted to lower frequencies, as observed in the FTIR spectrum of complex C2, and was associated to the delocalization of bonding electrons that occur in complexation. Higher frequencies observed for

Table 2. Synthesis of complex C1, C2 and C3.

Ligand			$CuCl_2.2H_2O$	
Code	**mMol**	**mg**	**mMol**	**mg**
L1	0.05	18.0	0.05	100.0
L2	0.18	58.0	0.18	31.0
L3	0.24	41.0	0.24	86.0

L1 = 3,4-methylenedioxybenzyl-*S*-benzyldithiocarbazate; L2 = *p*-chloro-benzyl-*S*-benzyldithiocarbazate; L3 = 2,6-dichlorobenzyl-*S*-benzyldithiocarbazate.

C1 and C3 were correlated to metal-nitrogen bond formation, which induced shorter C-N bond lengths.

The ligand acts as a bidentate sulphur-nitrogen chelating agent. The ligands (L1, L2 and L3) also showed absorption bands at 929, 948 and 933 cm^{-1}, that were attributed to ν(C=S) (Ali and Tafafder, 1997; Silverstein and Webster, 1997). The ν(C=S) observed in the spectrum of free ligand is shifted to the higher energy in the complexes (Table 1), thus supporting the thione bonding with metal ions, such as the sulfur atom of the C=S group forming a coordination site (Al-Amin et al., 2014).

This data together with the absence of hydrogen signal around δ 4.00 ppm in the NMR spectra related to sulfhydryl group confirm the ligands as thione tautomers (Beckford et al., 2011). In the ^{1}H NMR spectra of ligands was observed a signal at δ 4.5 ppm (2H) which was attributed to methylene of *S*-benzyldithiocarbazate and a signal at δ 7.8 to 8.2 ppm correlated to hydrogen of azomethine imine (Beckford et al., 2011). The presence of these signals is typical of shiff bases and contributes to confirm the formation of ligands. By means of spectroscopic data L1 was identified as 3,4-methylenedioxybenzyl-*S*-benzyldithiocarbazate, L2 as *p*-chloro-benzyl-*S*-benzyldithiocarbazate, and L3 as 2,6-dichloro-benzyl-*S*-benzyldithiocarbazate:

3,4-Methylenedioxybenzyl-*S*-benzyldithiocarbazate (L1): 88% yield. Melting point: 190-194 °C. ^{1}H NMR (DMSO-d_6) δ (ppm): 13.30 (NH, s, 1H); 8.15 (HC=N, s, 1H); 6.09 (OCH_2O, s, 2H); 4.48 (CH_2, s, 2H); 7.41 (H_m, ring B, d, 2H); 7.33 (H_o, ring B, t, 2H); 7.28 (Hp, ring B, d, 1H); 7.22 (H_o ring B, s, 1H); 7;17 (H_o, ring A, d, 1H); 6.99 (H_m, ring A, d, 1H).

***p*-Chloro-benzyl-*S*-benzyldithiocarbazate** (L2): 85% yield. Melting point: 150-154 °C. ^{1}H NMR ($CDCl_3$) δ (ppm): 10.45 (NH, s, 1H); 4.58 (CH_2, s, 2H); 7.85 (HC=N, s, 1H); 7.6 (H_m, ring A, d, 2H); 7.4 (H_o, ring A, d, 2H); 7.39-7.28 (ring B, m, 5H).

2,6-Dichloro-benzyl-*S*-benzyldithiocarbazate (L3): 86 % yield. Melting point: 168-172 °C. ^{1}H NMR ($CDCl_3$) δ (ppm): 10.62 (NH, s, 1H); 8.28 (CH, s, 1H); 4.57 (CH_2, s, 2H); 7.47-7.42 (ring A, m, 3H); 7.37 (H_m, ring B, d, 2H); 7.34 (H_o, ring B, t, 2H); 7.28 (H_p, ring B , t, 1H).

Regarding the complex formation, the following yields were obtained: 32 (C1), 24 (C2) and 20% (C3). By means of spectral data, the complexes were identified as $[Cu(L1)Cl_2{\cdot}2H_2O]$ (C1), $[Cu(L2)Cl_2{\cdot}2H_2O]$ (C2) and $[Cu(L3)Cl_2{\cdot}2H_2O]$ (C3). In comparison with the ligand L1, L2 and L3, the IR absorption bands of ν(C=N) and ν(C=S) of the respective complex C1, C2 and C3 occurred in longer wavelengths in the spectra (Table 3), indicating coordination of nitrogen and sulfur atoms with ion copper (II). By means of this result was possible to infer the formation of Cu(II) complex with an octahedral structure due to the nature of copper and the stereochemistry employed in the synthesis reaction (Figure 1).

The FTIR and UV-V is absorption bands of ligands L1, L2 and L3 compiled in Table 3, and physical properties of the Cu(II) complexes C1, C2 and C3 as shown in Table 4. The absorption band in the visible region UV-Vis spectra of these complexes was attributed to n→π* transition for the *S*-benzyldithiocarbazate moiety. Although the n→π* band of dithiocarbazate group also showed a blue shift (339 to 375 nm) in Cu(II) complexes (Tarafder et al., 2002a,b; Monika et al., 2014). The bathochromic shift observed in the UV-Vis spectra of Cu(II) complexes suggesting a structural change or electronic behavior associated to a selected transition. In the Cu(II) complexes, the band that is related to the possible transition $^2T_{2g} \leftarrow {}^2E_g$, and feature of a octahedral geometry was not observed.

In the electronic spectra of the complexes C1, C2 and C3, the absence of d-d transition, is due to the intrusion of tails of intense charge transfer bands into visible portion of the spectrum which masks the expected d-d bands, the tail of this band covers all d-d transition (Takjoo and Centore, 2013). In ligands containing sulphur atoms, the strong inter-ligands charge transfer transitions (S→M) interfere in the observation of π→π* bands which can be correlated to the azomethine group and ring (Takjoo and Centore, 2013). These results are in accordance with published data for similar complexes (Tarafder et al., 2002a,b; Ali et al., 2011). At room temperature were observed Bohr magneton (μB) for Cu(II) complex C1, C2 and C3 effective in the range of 1.7 to 2.1 μB corresponding to one unpaired electron, suggesting an octahedral environment. This behavior is expected for transition metals (3d9), as in this case with

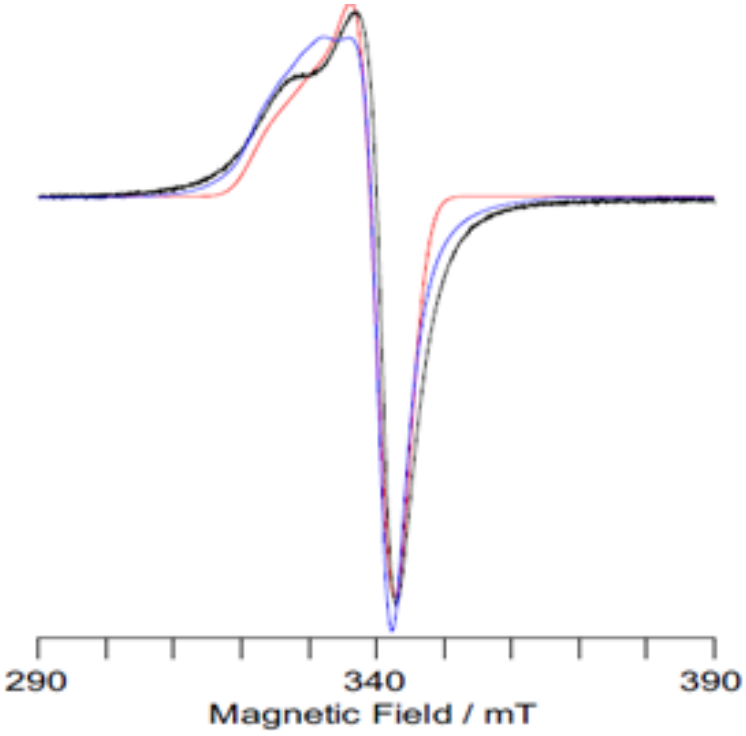

Figure 2. EPR spectra obtained for the powder of complex C1 $[Cu(L1)(Cl)_2(H_2O)_2]$ at 293 K (9.800 GHz) (Black line). Gaussian simulation (Red line) and Lorentzian simulation (Blue line).

the Cu(II) in dilute environment. The molar conductance of these complexes dissolved in DMSO is presented in Table 2. The low molar conductance values show that the metal complexes are non-electrolytes.

These results indicate that the complexes do not dissociate in this solvent because the values are very small compared with those expected for 1:1 electrolytes (Ali et al., 2011). In the EPR spectra (Figure 2), obtained at room temperature for complex C1, was observed a signal at 330 mT (3.3 $x10^7$ Gauss) (West and Liberta, 1993) that confirms the presence of Cu(II) in the structure.

The g values of the complex were obtained by means of simulation and the experimental results were 2.04, 2.05 and 2.13, respectively correspondent to g_x and g_y y g_z. For constant A_x, A_y and A_z were 10, 10 and 90, respectively. Based on the values obtained for g_z (2.13) and A_z (90), it was determined that complex C1 has an elongated octahedral structure (Geary, 1971; West and Liberta, 1993). Having gx and gy, it is suggested that this complex is a slight rhombic distortion octahedral (Geary, 1971; West and Liberta, 1993; Hamid et al., 2009). These values differ from those previously reported for this type of structure. However, the observed differences is herein attributed due to the published data were obtained at temperatures below 100 K (Hamid et al., 2009; Garribba and Micera, 2006), thus the working temperature affects the behavior of the analyzed molecule.

Antimicrobial activity

Regarding ligand L1, L2 and L3 were not observed activity against bacteria *E. coli.* Nevertheless, the complexes inhibit the growth of this bacterium, with MIC of C1 ≥ 15 µg/mL, C2 ≥ 150 µg/mL and C3 ≥ 200 µg/mL. The complex C1 induced growth inhibition of *S. aureus* at ≥ 50 µg/ml and of *C. albicans* at ≥ 15 µg/mL (Table 5). In the assays with *S. cerevisiae* , were observed inhibition activity induced by C1 at ≥ 15 µg/mL and C2 ≥ 50 µg/mL (Table 5). These results suggest C1 as compound with higher inhibitory property than C2 and C3. This fact can be attributed to the interaction between the binder whose structure has electron donor atoms (N and S), and also has the dioxolane ring B (Figure 1).

The presence of oxygen atoms completing the five member ring with carbons of benzyl group has being studied indicating that they influence the activity of both ligands as its metal complexes with Ni(II) and Sn(II) (Ali et al., 2008; Muhammad et al., 2010). In this study the higher activity presented by complex C1 probably occurred due to the presence of two oxygen atoms in its structure (Table 5).

***In silico* activity prediction**

By means of ChemMapper and PASSonline tools were

Table 3. FTIR and UV-Vis spectral data of ligand L1, L2 and L3, and respective Cu(II) complex C1, C2 and C3, respectively.

Compound	Absorption band				
	IR-TF (cm^{-1})				UV-Vis
	υNH	υC-N; N-N	υC=N	υC=S	λmáx nm (log ε) $Lmol^{-1}cm^{-1}$
Ligand					
L1	3128	1597	1450	929	350 (4.46)
L2	3097	1597	1485	948	336 (4.46)
L3	3124	1577	1423	933	332 (4.40)
Cu(II) complex					
C1	3200	1620	1497	964	355 (3.97)
C2	2981	1593	1485	966	375 (4.03)
C3	3240	1620	1427	972	339 (3.88)

Table 4. Physical properties of Cu(II) complex C1, C2 and C3.

Complex	Chemical formula	Color	m.p[a]	μB[b]	Λ[c]
C1	$[Cu(L1)Cl_2 \cdot 2H_2O]$	Light brown	170-172	1.76	56.5
C2	$[Cu(L2)Cl_2 \cdot 2H_2O]$	Yellow	176-182	2.1	13.7
C3	$[Cu(L3)Cl_2 \cdot 2H_2O]$	Yellow	>50*	1.9	30.8

[a]Melting point °C (* With decomposition); [b] Bohr magneton at 293 K; [c] Molar conductance (Ω^{-1} cm^2 mol^{-1}), 10^{-3} M in DMSO solution.

Table 5. Minimun inhibitory concentration (MIC) of the ligands L1, L2, L3 and complexes de Cu(II).

Microorganism	Minimum inhibitory concentration (μg/mL) of the compounds					
	L1	L2	L3	C1	C2	C3
E. coli	-	-	-	> 15	> 150	> 200
S. aureus	-	-	-	> 50	-	-
C. albicans	-	-	-	> 15	-	-
S. cerevisiae	-	-	-	> 15	> 50	-

[–] Indicates no observed activity in the concentration range evaluated.

not possible to observe *in silico* predictions for Cu(II) complex C1, C2 and C3. This fact may be associated to the absence of similar compounds tested and available biological effect information, or to the low similarity with active compounds available in the libraries evaluated mainly with the aid of this tool. Using the PASSonline tool were not observed prediction of adverse effect for ligands L1, L2 and L3 related to abortion inducer, arrhythmogenic, bronchoconstrictor, carcinogenic, cardiotoxic, convulsant, cytotoxic, DNA damaging, depression, embryotoxic, emetic, eye irritation, hallucinogen, hepatotoxic, hypo- or hypercalcaemic, hypercholesterolemic, hyperglycemic, hypertensive, hyperthermic, hypnotic, hypokalemia, hypothermic, narcotic, nephrotoxic, neurotoxic, QT interval prolongation, rubefacient, sedative, sensitization, skin irritation, spasmogenic, mutagenic, teratogen, thrombocytopoiesis inhibitor, torsades de pointes, toxic for respiratory center, vasodilator and vasopressor.

However, antibacterial, antimycobacterial, antituberculosis and anti-infective activities were directly predicted by PASSonline. Other effects, such as protease inhibitor (Doumas et al., 2005; Habib and Fazili, 2007; Kimet al., 2009), glutamylendopeptidase II inhibitor (Supuran et al., 2002), beta lactamase inhibitor (Brown et al., 1976) and GABA B receptor agonist (Tsuji et al., 1988) were also established (Table 6). Antiparasitic activity related to Falcipain inhibitor (Rosenthal, 2011; Marco and Coterón, 2012), Falcipain 2 inhibitor (Ettari et al., 2010), Falcipain 3 inhibitor (Rosenthal, 2011), PfA-M1 aminopeptidase inhibitor (Flipo et al., 2007), and antiprotozoal effect (Coccidial, Histomonas, Babesia,

Table 6. *In silico* test prediction of potential biologic effect of ligand L1, L2 and L3 found using PASSonline* tool.

Target	Ligand		
	L1(179*)	L2 (363*)	L3 (863*)
PfA-M1 aminopeptidase inhibitor	0.598	0.587	0.643
Antiviral -Picornavirus	0.246	0.486	0.626
Antituberculosic	0.301	0.336	0.486
Cytoprotectant	0.110	0.435	0.529
Antimycobacterial	0.259	0.306	0.464
Falcipain 3 inhibitor	0.292	0.309	0.410
Antiprotozoal -Coccidial	0.291	0.307	0.314
Cytidine deaminase inhibitor	0.298	0.293	0.295
Glutamyl endopeptidase II inhibitor	0.058	0.301	0.477
Beta-adrenergic receptor kinase inhibitor	0.077	0.217	0.533
Protease inhibitor	0.246	0.234	0.324
Anti-Helicobacterpylori	0.264	0.206	0.263
Falcipain 2 inhibitor	0.193	0.163	0.199
Falcipain inhibitor	0.193	0.163	0.199
Beta lactamase inhibitor	0.104	0.122	0.233
Antiinfective	0.118	0.020	0.074
Antiprotozoal -Histomonas	0.047	0.063	0.099
GABA aminotransferase inhibitor	0.271	-	0.056
Antiviral -Influenza	0.072	-	0.191
Antibacterial	0.076	-	0.179
GABA B receptor agonist	-	0.137	0.106
Antiviral -Adenovirus	0.137	-	0.096
Antiprotozoal -Babesia	-	0.048	0.169
Transcription factor inhibitor	0.100	-	0.071
Antiprotozoal -Trichomonas	-	-	0.183
Antiprotozoal -Trypanosoma	0.147	-	-
GABA C receptor agonist	-	-	0.070

* - nº of biological effect predicted by PASSonline

Trichomonas and Trypanosoma) were adequately predicted by this tool. The PASSonline tool indicate antiviral activity against *Picornavirus*, *Helicobacter pylori*, *Influenza* and *Adenovirus* (Table 6). In Table 6 were compiled the potential biological effects predicted by PASSonline web tool at least for the ligands L1, L2 and L3, and that directly correlate the anti-parasitic, antiviral and antimicrobial activities.

By means of ChemMapper tool were predicted antiviral and antitumor activities for the targets beta-1 adrenergic receptor (Hjalmarson et al., 2002), beta-2 adrenergic receptor (Irwin et al, 1990), cellular tumor antigen P53 (Cuff and Ruby, 1996), cyclin-A2 (Cribier et al., 2013), 5-hydroxytryptamine 1A receptor (Fiorino et al., 2014), cell division protein kinase 2 (Chow et al., 2009) and collagenase 3[MMP-13] (Casini et al., 2002), proto-oncogene tyrosine-proteinkinase LCK (Hansen et al., 2010), pyruvate dehydrogenase [cytochrome] (Ganapathy-Kanniappan et al., 2009) and ribosyldihydronicotinamidede hydrogenase [quinone] (Dolai et al., 2011), thymidylatesynthase (Balzarini, et al., 1987) (Table 7). The target trypsin beta indicated by ChemMapper tool is associated to bacterial infectious diseases, and the target glutathionereductase is associated to parasitic diseases. Based on the results was possible to deduce that ligand L1, the Schiff base that originate complex C1, present significant similarity with compounds that acts as inhibitors of trypsin-beta (Table 7) which is involved in the growth of bacteria. The chemical structure of ligand L2 and L3 is similar to compounds that induce the inhibition of thymidylate synthase (Table 7). This enzyme is related to the conversion of folic acid to dihydrofolate (DHF) and then to tetrahydrofolate (THF) which is directly involved in the synthesis of bacterial DNA.

Conclusion

Three new ligands L1, L2 and L3 derivatives of *S*-

Table 7. *In silico* test prediction of potential biologic targets of ligand L1, L2 and L3 found using ChemMapper** tool.

Biological target	Ligand		
	L1	L2	L3
ATP-binding cassette transporter sub-family C member 8	0.63	0.65	0.67
Cell Division Protein Kinase 2	0.62	0.64	0.68
Collagenase 3, MMP-13	0.62	0.61	0.65
Sodium channel protein type 5 subunit alpha	-	0.63	0.66
5-hydroxytryptamine 1A receptor	-	-	0.62
5-hydroxytryptamine 1B receptor	-	-	0.62
Albendazole monooxygenase	0.63	-	-
Amine Oxidase [Flavin-Containing] B	-	0.63	-
Arylamine N-acetyltransferase	-	-	0.62
Beta-1 adrenergic receptor	-	-	0.62
Beta-2 adrenergic receptor	-	-	0.62
Cellular Tumor Antigen P53	0.60	-	-
Cyclin-A2	-	0.60	0.63
elastase	-	-	0.61
Enoyl-[acyl-carrier-protein] reductase [NADH]	-	-	0.60
Glutathione reductase	-	-	0.63
Hemoglobin subunit alpha	-	-	0.60
Hydrolases (Acting on carbon-nitrogen bonds, other than peptide bonds, in linear amides)	-	-	0.62
Malate dehydrogenase	-	-	0.63
Myoglobin	-	-	0.60
Proto-oncogene tyrosine-protein kinase LCK	-	-	0.62
Pyruvate dehydrogenase [cytochrome]	-	-	0.63
Ribosyldihydronicotinamide dehydrogenase [quinone]	0.63	-	-
Thymidylate synthase	-	0.69	0.67
Trypsin beta	0.61	-	-

[---] Absence of similar ligands in the data base

benzyldithiocarbazate and its Cu(II) complexes C1, C2 and C3 were synthesized with a good yield, and its chemical structures were identified by means of its respective IR and ^{1}H NMR data. Through the spectral data was established that both in solid as in solution, the ligands have thione tautomer form. The structure of complex C1 in solid state was confirmed by EPR, at room temperature. Complex C1 showed the major *in vitro* antimicrobial activity. The bacterial inhibition effect was observed for all microorganism subjected to assays. The inhibition property was attributed mainly to the metal-ligand interaction and probably by the presence of two oxygen atoms in the structure of C1, commonly found in active compounds. This study results contribute to future studies of similar complexes involving quantitative structure-activity relationships (QSAR).

ACKNOWLEDGEMENTS

The authors wish to thank the Dirección de Investigación Sede Bogotá (DIB) of Universidad Nacional de Colombia by financial support (N°. 201010016735), and to Dr. Ovidio Almanza of Laboratorio de EPR, Departamento de Física, of Universidad Nacional de Colombia.

Conflict of Interests

The authors have not declared any conflict of interests.

REFERENCES

Al-Amin M, Islam AA, Sheikh MC, Alam MS, Zangrando E, Alam MA, Tarafder MTH, Miyatake R (2014). Synthesis, characterization and bio-activity of a bidentate NS Schiff base of S-allyldithiocarbazate and its divalent metal complexes: X-ray crystal structures of the free ligand and its nickel(II) complex. Trans. Met. Chem. 39:141-149.

Alanne AL, Lahtinen M, Löfman M, Turhanen P, Kolehmainen E, Vepsäläinen J, Sievänen E (2013). First bisphosphonate hydrogelators: potential composers of biocompatible gels. J. Mater. Chem. B. 1:6201-6212.

Ali MA, Tarafder MTH (1977). Metal complexes of sulphur and nitrogen-containing ligands: Complexes of S-benzyldithiocarbazate and a schiff base formed by its condensation with pyridine-2-carboxa ldehyde. J. Inorg. Nucl. Chem. 39(10):1785-1791.

Ali MA, Bakar HJHA, Mirza AH, Smith SJ, Gahan LR, Bernhardt PV (2008). Preparation, spectroscopic characterization and X-ray crystal and molecular structures of nickel(II), copper(II) and zinc(II) complexes of the Schiff base formed from isatin and

S–methyldithiocarbazate (Hisa–sme). Polyhedron. 27:71-79.
Ali MA, Mirza AH, Ting WY, Hamid MHSA, Bernhardt PV. Butcher RJ (2012). Mixed-ligand nickel(II) and copper(II) complexes of tridentate ONS and NNS ligands derived from S-alkyldithiocarbazates with the saccharinate ion as a co-ligand. Polyhedron 48:167-173.
Ali MA, Mirza AH, Butcher RJ, Bernhardt PV, Karim MR (2011). Self-assembling dicopper(II) complexes of di-2-pyridyl ketone Schiff base ligands derived from S-alkyldithiocarbazates. Polyhedron 30(9):1478-1486.
Balzarini J, Clercq E, Verbruggen A, Ayusawa D, Shimizu K, Seno T (1987). Thymidylate synthase is the principal target enzyme for the cytostatic activity of (E)-5-(2-bromovinyl)-2'-deoxyuridine against murine mammary carcinoma (FM3A) cells transformed with the *Herpes simplex virus* type 1 or type 2 thymidine kinase gene. Mol. Pharmacol. 32(3):410-416.
Bauer AW, Kirby EM (1966). Antibiotic susceptibility testing by standardized single disk method. Am. J. Clin. Pathol. 45:493-496.
Beckford F, Dourth D, Shaloski M, Didion J, Thessing J, Woods J, Crowell V, Gerasimchuk N, Gonzalez-Sarrías A, Seeram NP (2011). Half-sandwich ruthenium–arene complexes with thiosemicarbazones: Synthesis and biological evaluation of [(η6 -p-cymene)Ru(piperonalthiosemicarbazones)Cl]Cl complexes. J. Inorg. Biochem. 105:1019-1029.
Beraldo H (2004). Semicarbazonas e tiossemicarbazonas: o amplo perfil farmacológico e usos clínicos. Quím. Nova. 27(3):461-471.
Brown AG, Butterworth D, Cole M, Hanscomb G, Hood JD, Reading C, Rolinson GN (1976). Naturally-occurring β-lactamase inhibitors with antibacterial activity. J. Antibiot. 29(6):668-669.
Casini A, Scozzafava A, Supuran CT (2002). Sulfonamide derivatives with protease inhibitory action as anticancer, anti-inflammatory and antiviral agents. Expert Opin. Ther. Patents. 12(9):1307-1327.
Chen D, Milacic V, Frezza M, Dou QP (2009). Metal complexes, their cellular targets and potential for cancer therapy. Curr. Pharm. Des. 15(7):777-791.
Chow WA, Jiang C, Guan M (2009). Anti-HIV drugs for cancer therapeutics: back to the future?. Lancet. Oncol.10(1): 61–71.
Cribier A, Descours B, Valadão ALC, Laguette N, Benkirane M (2013). Phosphorylation of SAMHD1 by Cyclin A2/CDK1 Regulates Its Restriction Activity toward HIV-1. Cell Rep. 3(4):1036–1043.
Cuff S, Ruby J (1996). Evasion of apoptosis by DNA viruses. Immunol. Cell Biol. 74:527-537.
Dolai S, Xu Q, Liu F, Molloy MP (2011). Quantitative chemical proteomics in small-scale culture of phorbol ester stimulated basal breast cancer cells. Proteomics. 11(13):2683-2692
Doumas S, Kolokotronis A, Stefanopoulos P (2005). Anti-Inflammatory and Antimicrobial Roles of Secretory Leukocyte Protease Inhibitor. Infect. Immun. 73(3):1271-1274.
Esmaielzadeh S, Azimian L, Shekoohi K, Mohammadi K (2014). Coordination chemistry, thermodynamics and DFT calculations of copper(II) NNOS Schiff base complexes. Spectrochim. Acta Part A Mol. Biomol. Spectrosc.133:579-590.
Ettari R, Bova F, Zappalà M, Grasso S, Micale N (2010). Falcipain-2 inhibitors. Med. Res. Rev. 30(1):136-167.
Filimonov DA, Lagunin AA, Gloriozova TA, Rudik AV, Druzhilovskii DS, Pogodin PV, Poroikov VV (2014). Prediction of the Biological Activity Spectra of Organic Compounds Using the Pass Online Web Resource. Chem. Heterocycl. Compd. 50(3):444-457.
Fiorino F, Severino B, Magli E, Ciano A, Caliendo G, Santagada V, Frecentese F, Perissutti E (2014). 5-HT1A Receptor: An Old Target as a New Attractive Tool in Drug Discovery from Central Nervous System to Cancer. J. Med. Chem. 57(11):4407-4426.
Flipo M, Beghyn T, Leroux V, Florent I, Déprez B, Deprez-Poulain R (2007). Novel selective inhibitors of the zinc plasmodial aminopeptidase PfA-M1 as potential antimalarial agentes. J. Med. Chem. 50(6):1322-1334.
Ganapathy-Kanniappan S, Geschwind J-FH, Kunjithapatham R, Buijs M, Vossen JA, Tchernyshyov I, Cole RN, Syed LH, Rao PP, OtA S, Vali M (2009). Glyceraldehyde-3-phosphate Dehydrogenase (GAPDH) is Pyruvylated during 3-Bromopyruvate Mediated Cancer Cell Death. Anticancer. Res. 29(12):4909-4918.
Garoufis A, Hadjikakou SK, Hadjiliadis N (2009). Review Palladium coordination compounds as anti-viral, anti-fungal, anti-microbial and anti-tumor agents. Coord. Chem. Ver. 253:1384-1397.
Garribba E, Micera G (2006). The determination of the geometry of Cu(II) complexes. An EPR spectroscopy experiment. J. Chem. Educ. 83(8):1229-1232.
Geary WJ (1971). The use of conductivity measurements in organic solvents for the characterization of coordination compounds. Coord Chem Rev. 7:81-122.
Gong J, Cai C, Liu X, Ku X, Jiang H, Gao D, Honglin L (2013a). ChemMapper: a Versatile Web Server for Exploring Pharmacology and Chemical Structure Association Based on Molecular 3D Similarity Method. Bioinformatics. 29(14):1827-1829.
Gong J, Cai CH, Liu X, Ku X, Jiang H, Gao D, Li H (2013b). ChemMapper: a Versatile Web Server for Exploring Pharmacology and Chemical Structure Association Based on Molecular 3D Similarity Method. Bioinformatics. 29(14):1827-1829.
Habib H, Fazili KM (2007). Plant protease inhibitors: a defense strategy in plants. Biotechnol. Mol. Biol. Rev. 2:68-85.
Hamid MHSA, Ali MA, Mirza AH, Bernhardt PV, Moubaraki B, Murray KS (2009). Magnetic, spectroscopic and X-ray crystallographic structural studies on copper(II) complexes of tridentate NNS Schiff base ligands formed from 2-acetylpyrazine and S–methyl–and S–benzyldithiocarbazates. Inorg. Chim. Acta. 362:3648–3656.
Hansen TR, Smirnova NP, Campen HV, Shoemaker ML, Ptitsyn AA, Bielefeldt-Ohmann H (2010). Maternal and fetal response to fetal persistent infection with bovine viral diarrhea virus. Am. J. Reprod. Immunol. 64(4):295-306.
Hjalmarson A, Fu M, Mobini R (2002). Who are the enemies? Inflammation and autoimmune mechanisms. Eur. Heart J. 4(G):G27–G32.
How N-F, Crouse KA, Tahir IM, Tarafder MTH, Cowley AR (2008). Synthesis, characterization and biological studies of S-benzyl-b-N-(benzoyl) dithiocarbazate and its metal complexes. Polyhedron. 27:3325-3329.
Irwin M, Hauger RL, Jones L, Provencio M, Britton KT (1990). Sympathetic nervous system mediates central corticotropin-releasing factor induced suppression of natural killer cytotoxicity. J. Pharmacol. Exp. Ther. 255(1):101-107.
Islam AA, Sheikh MC, Alam MS, Zangrando E, Alam MA,Tarafder MTH, Miyatake R (2014). Synthesis, characterization and bio-activity of a bidentate NS Schiff base of S-allyldithiocarbazate and its divalent metal complexes: X-ray crystal structures of the free ligand and its nickel(II) complex. Transition Met Chem. 39:141-149.
Islam AA, Tarafder MTH, Sheikh MC, Alam MA, Zangrando E (2011). Coordination chemistry of [methyl-3-(4-benzyloxyphenyl)methylene]dithiocarbazate with divalent metal ions: crystal structures of the *N*,*S* Schiff base and of its bis-chelated nickel(II) complex. Transition Met. Chem. 36(5):531-537.
Kelland L (2007). The resurgence of platinum-based cancer chemotherapy. Nat Rev. Cancer. 7(8):573-584.
Kim JY, Park SC, Hwang I, Cheong H, Nah JW, Hahm KS, Park Y (2009). Protease inhibitors from plants with antimicrobial activity. Int. J. Mol. Sci. 10:2860-2872.
Lagunin A, Stepanchikova A, Filimonov D, Poroikov V (2000). Pass: prediction factivity spectra for biologically active substances. Bioinformatics. 16(8):747-748.
Lagunin A, Filimonov D, Poroikov V (2010). Multi-targeted natural products evaluation based on biological activity prediction with PASS. Curr. Pharm. Des. 16(15):1703-1717.
Liu X, Jiang H, Li H (2011). SHAFTS: A Hybrid Approach for 3D Molecular Similarity Calculation. 1. Method and Assessment of Virtual Screening. J. Chem. Inf. Model. 51(9):2372-2385.
Lu W, Liu X, Cao X, Xue M, Liu K, Zhao Z, Shen X , Jiang H, Xu Y, Huang J, Li H (2011). SHAFTS: A Hybrid Approach for 3D Molecular Similarity Calculation. 2. Prospective Case Study in the Discovery of Diverse p90 Ribosomal S6 Protein Kinase 2 Inhibitors to Suppress Cell Migration. J. Med. Chem. 54:3564-3574.
Marco M, Coterón JM (2012). Falcipain inhibition as a promising antimalarial target. Curr. Top. Med. Chem. 12(5):408-444.
Monika M, Karishma T, Singh AK, Singh VP (2014). Synthesis, structural and corrosion inhibition studies on Mn(II), Cu(II) and Zn(II) complexes with a Schiff base derived from 2-hydroxypropiophenone. Polyhedron. 77:57-65.

Muhammad H, Mukhtiar H, Ali SA, Bhatti MH, Ahmed MS, Mirza B, Stoeckli-Evans H (2010). *In vitro* biological studies and structural elucidation of organotin(IV) derivatives of 6-nitropiperonylic acid: Crystal structure of $\{[(CH_2O_2C_6H_2(o\text{-}NO_2)COO)SnBu_2]_2O\}_2$. Polyhedron. 29:613-619.

Mysinger MM, Carchia M, Irwin JJ, Shoichet BK (2012). Directory of useful decoys, enhanced (DUD-E): better ligands and decoys for better benchmarking. J. Med.Chem. 55:6582-6594.

Nanjundan N, Selvakumar P, Narayanasamy R, Haque RA, Velmurugan K, Nandhakuma R, Silambarasan T, Dhandapani R (2014). Synthesis, structure, DNA/BSA interaction and *in vitro* cytotoxic activity of nickel(II) complexes derived from S-allyldithiocarbazate. J. Photochem. Photobiol. Biol. 141:176-185.

Ott I (2009). Review: On the medicinal chemistry of gold complexes as anticancer drugs. Coord. Chem. Rev. 253(11-12):1670-1168.

Ravoof TBSA, Crouse KA, Tahir IM, Cowley AR, Ali MA (2004). Synthesis, characterization and bioactivity of mixed-ligand Cu(II) complexes containing S-methyldithiocarbazate derivatives and saccharinate ligands and the X-ray crystal structure of the copper–saccharinate complex containing S-methyl-β-N-(6-methylpyrid-2-yl)methylenedithiocarbazate. Polyhedron 23:2491–2498.

Ravoof TBSA, Crouse KA, Tahir IM, Cowley AR, Ali MA (2007). Synthesis, characterization and bioactivity of mixed-ligand Cu(II) complexes containing Schiff bases derived from S-benzyldithiocarbazate and saccharinate ligand and the X-ray crystal structure of the copper-saccharinate complex containing S-benzyl-β-N-(acetylpyrid-2-yl)methylenedithiocarbazate. Polyhedron 26:1159-1165.

Rigol C, Olea-Azar C, Mendizábal F, Otero L, Gambino D, González M, Cerecetto H (2005). Electrochemical and ESR study of 5-nitrofuryl-containing thiosemicarbazones antiprotozoal drugs. Spectrochim. Acta, Part A. 61(13-14):2933-2938.

Rosenthal PJ (2011). Falcipains and other cysteine proteases of malaria parasites. Adv. Exp. Med. Biol. 712:30-48.

Silverstein RM, Webster FX (1997). Spectrometric Identification of Organic Compounds. 6th ed. Willey: London.

Supuran CT, Scozzafava A, Clare BW (2002). Bacterial protease inhibitors. Med. Res. Rev. 22(4):329-372.

Takjoo R, Centore R (2013). Synthesis, X-ray structure, spectroscopic properties and DFT studies of some dithiocarbazate complexes of nickel(II). J. Mol. Struct. 1031:180-185.

Tamayo LV, Burgos AE, Brandão PFB (2014). Synthesis, characterization, and antimicrobial activity of the ligand 3-methylpyrazole-4-carboxaldehyde thiosemicarbazone and its Pd(II) complex. Phosphorus, Sulfur Silicon Relat. Elem. 189:52-59.

Tarafder MTH, Ali AM, Wong YW, Wong SH, Crouse KA (2001). Complexes of transition and nontransition metals of dithiocarbazate ion and their biological activities. Synth. React. Inorg. Met.-Org. Chem. 31(1):115-125.

Tarafder MTH, Khoo T-J, Crouse KA, Ali AM, Yamin BM, Fun H-K (2002a). Coordination chemistry and bioactivity of some metal complexes containing two isomeric bidentate NS Schiff bases derived from S-benzyldithiocarbazate and the X-ray crystal structures of S-benzyl-β-N-(5-methyl-2-furylmethylene)dithiocarbazate and bis[S-benzyl-β-N-(2-furylmethylketone)dithiocarbazato]cadmium(II). Polyhedron 21(27-28):2691-2698.

Tarafder MTH, Khoo TJ, Crouse KA, Ali AM, Yamin BM, Fun H-K (2002b). Coordination chemistry and bioactivity of Ni^{2+}, Cu^{2+}, Cd^{2+} and Zn^{2+} complexes containing bidentate Schiff bases derived from S-benzyldithiocarbazate and the X-ray crystal structure of bis[S-benzyl-β-N-(5-methyl-2-furylmethylene)dithiocarbazato]cadmium(II). Polyhedron 21(25-26):2547-2554.

Tsuji A, Sato H, Kume Y, Tamai I, Okezaki E, Nagata O, Kato H (1988). Inhibitory effects of quinolone antibacterial agents on gamma-aminobutyric acid binding to receptor sites in rat brain membranes. Antimicrob. Agents Chemother. 32(2):190-194.

Wang X, Chen H, Yang F, Gong J, Li S, Pei J, Liu X, Jiang H, Lai L, Li H (2014). Drug: A web-accessible and interactive drug discovery and design platform. J. Chemom. 6:28.

West DX, Liberta AE (1993). Thiosemicarbazone complexes of copper(II): structural and biological studies. Coord. Chem. Rev. 123:49-71.

Zangrando E, Islam MT, Islam AA, Sheikh MC, Tarafder MTH, Miyatake R, Zahan R, Hossain MA (2015). Synthesis, characterization and bio-activity of nickel(II) and copper(II) complexes of a bidentate NS Schiff base of S-benzyl dithiocarbazate. Inorg. Chim. Acta. 427:278-284.

Ziessel R (2001). Schiff-based bipyridin ligands. Unusual coordination features and mesomorphic behaviour. Coord. Chem. Rev. 216:195-223.

African Journal of Pharmacy and Pharmacology

Related Journals Published by Academic Journals

- *Journal of Medicinal Plant Research*
- *African Journal of Pharmacy and Pharmacology*
- *Journal of Dentistry and Oral Hygiene*
- *International Journal of Nursing and Midwifery*
- *Journal of Parasitology and Vector Biology*
- *Journal of Pharmacognosy and Phytotherapy*
- *Journal of Toxicology and Environmental Health Sciences*

academicJournals